

Soft Condensed Matter Physics

T.C. Lubensky

Department of Physics and Astronomy, University of Pennsylvania, Philadelphia, PA 19104

(November 26, 2024)

Soft condensed matter physics is the study of materials, such as fluids, liquid crystals, polymers, colloids, and emulsions, that are “soft” to the touch. This article will review some properties, such as the dominance of entropy, that are unique to soft materials and some properties such as the interplay between broken-symmetry, dynamic mode structure, and topological defects that are common to all condensed matter systems but which are most easily studied in soft systems.

I. INTRODUCTION

In recent years soft condensed matter physics, or simply soft physics, has emerged as an identifiable subfield of the broader field of condensed matter physics. As its title implies, it is the study of matter that is “soft,” i.e., of materials that will not hurt your hand if you hit them. This is in contrast to “hard” materials such as aluminum or sodium chloride that are generally associated with the field of solid state physics. Though the term soft physics has only recently gained acceptance, its purview is vast. It subsumes all of fluid physics, including both microscopic structure and macroscopic phenomena such as hydrodynamic flow and instabilities. It includes liquid crystals and related materials with their vast variety of broken-symmetry states. It includes colloids, emulsions, microemulsions, membranes, and a large fraction of biomaterials. It is a field that presents fundamental scientific challenges and one that has substantial economic impact. In this article, I will give a brief overview of some fundamental problems of soft condensed matter physics [1].

The defining property of soft materials is the ease with which they respond to external forces. This means not only that they distort and flow in response to modest shears but also that thermal fluctuations play an important if not dominant role in determining their properties. They cannot be described simply in terms of harmonic excitations about a quantum ground state as most hard materials can. There are soft materials that possess virtually every possible symmetry group, including three-dimensional crystalline symmetries normally associated with hard materials and many others not found at all in hard materials. Ordered phases of soft materials can easily be distorted, making it possible to study and to control states far from equilibrium or riddled with defects. Thus, soft materials offer an ideal testing ground for fundamental concepts, involving the connection between symmetry, low-energy excitations, and topological defects, that are at the very heart of physics.

In this article, I will discuss four broad problems that reflect the richness of soft physics: entropic forces and entropically induced order, broken symmetries, topological defects, and membranes. This is by no means an exhaustive list; it does not, for example, include nonequilibrium and non-linear phenomena or the vast field of polymer

physics; it is, however, a list that has general applicability to hard as well as soft physics.

II. THE TRIUMPH OF ENTROPY

A. Introduction

Phases in thermodynamic equilibrium correspond to minima of the free energy $F = E - TS$, where E is the internal energy, T is the temperature, and S is the entropy. In hard materials, E tends to dominate over entropy: to a good approximation, internal energy determines the structure of equilibrium phases, and thermal fluctuations can be treated as perturbations about a minimum-energy phase. In soft systems, quite the opposite may be true: internal energy may either be small compared to TS , or it may not depend at all on configurational changes of the system. In the latter case, equilibrium states are those that maximize the entropy rather than minimize the internal energy. In addition, deviations of the entropy from its equilibrium maximum value create forces whose effects are every bit as real as those arising from the gradient of a potential. Perhaps the most familiar of such entropic forces is that required to stretch a polymer [2]. A polymer can be modeled as a sequence of N freely joined segments of length l . The entropy of such a chain is a maximum if it is completely unconstrained. Constraining its ends to have a separation R leads to an entropy reduction of $\Delta S = -3R^2/(2Nl^2)$, a free energy increase of $\Delta F = 3TR^2/(2Nl^2)$, and a force $f = -\partial F/\partial R = -3TR/(2Nl^2)$. In this section, we will explore some systems where entropy determines structure and interparticle forces.

B. Hard Spheres

The interaction potential between spherical atoms such as the noble gases consists of a long-range Van der Waals attractive part and a short-range repulsive part arising largely from the Pauli principle. Though the formation of crystals at low-temperature depends critically on the

existence of the attractive part of the potential, the properties of the liquid phases are determined to a large degree by the repulsive part, which is well modeled by a hard-sphere interaction that is infinite for interparticle separations less than the particles' diameter and zero otherwise. The hard-sphere gas was originally introduced as a mathematically simple model to describe fluid phases. Colloidal dispersions [3] of polystyrene spheres with radii ranging from $0.07\mu\text{m}$ to $4\mu\text{m}$ now provide nearly perfect experimental realizations of hard-sphere models. They provide marvelous laboratories in which to test a variety of theoretical predictions. They have also provided unexpected results.

In a hard-sphere system, the internal energy is zero in every allowed configuration. Interparticle forces and the free energy are determined entirely by entropy, which depends on the fraction ϕ of the total volume occupied by the hard spheres. At low volume fraction, collisions between particles are rare, and the system is an ideal gas. As volume fraction increases, particle motion is increasingly restricted by collisions with neighbors. At close-packing densities, all particle motion is arrested. A remarkable feature of hard-sphere systems is that there are two close-packing densities: the hexagonal-close-packing density, $\phi_h = 0.7405$, and the random close-packing density, $\phi_c = 0.638$. At random close-packing, there is a random arrangement of particles such that every particle has contacts with other particles that prevent its motion. It is important that $\phi_c < \phi_h$. Imagine expanding a hexagonal-close-packed lattice so that its lattice structure is maintained. Under this expansion, ϕ will decrease, and each particle will move freely in a cage centered at a lattice site of the expanded lattice. Because the particles are free to move, they have a nonzero entropy. Thus, such an expanded lattice at $\phi = \phi_c$ will clearly have a higher entropy than the random-close packed structure of the same volume fraction [4]. This implies that as volume fraction is increased from the liquid phase, it becomes entropically favorable for the system to form a periodic crystal rather than a random fluid structure: there is an entropically driven first-order liquid-to-solid transition [5,6]. On the phase boundary, a liquid with volume fraction 0.495 coexists with an FCC crystal with volume fraction 0.545.

Colloidal crystals have extremely small shear moduli compared to hard solids. Since the only energy in the problem is the temperature T , dimensional analysis dictates that the shear modulus μ must be of order $k_B T/v_0$ where v_0 is the free volume per particle, which is of order $(\phi - \phi_h)a^3 \approx 0.1a^3$ where a is the lattice spacing. For a somewhat less than a micron, this yields $\mu \sim 1$ dyne/cm², 10^{12} times smaller than for a hard solid like aluminum!. In charged colloids, Coulomb interactions will increase μ . The small value of μ makes it possible to study phenomena like shear melting of a crystal [7].

Mixtures of hard spheres of different sizes provide compelling examples of the power of entropy. Consider first mixtures of large spheres with radius $a_L \approx 4\mu\text{m}$ and

small spheres with radius $a_S \approx 0.1\mu\text{m}$. At comparable volume fractions, there will be far more small spheres than large spheres, and the entropy of the small spheres will dominate. Thus to a good approximation, the large spheres will adopt those configurations that maximize the entropy of the small spheres. The volume excluded to small spheres in the presence of two large spheres is smaller if the two spheres touch than if they are far apart as shown in Fig. 1. Thus, there is an entropically induced attractive force between the large spheres [8]. This is called a *depletion* force. It is of considerable importance in colloids and emulsions and in biological systems [9]. The particles involved do not have to be hard spheres. The small particle could, for example, be a polymer [10] or a micelle.

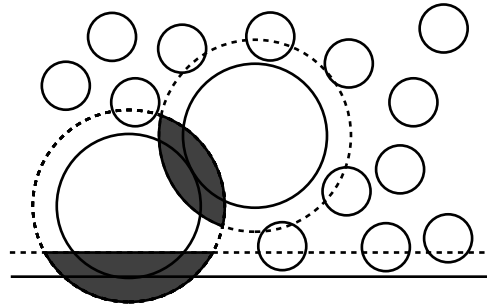


FIG. 1. Drawing of two large spheres, small spheres, and a wall. The full lines indicate the hard-sphere radii of the spheres. The dotted lines indicate the volume around an *isolated* large sphere or the isolated wall that centers of small spheres cannot enter. The shaded regions indicate the additional volume available to small spheres when two large spheres touch or when a large sphere touches a wall relative to the volume available when large spheres are far from each other and from any walls.

There is more free volume available to small particles if a large particle is in contact with the surfaces of a container than if it is removed from that surface. There is thus an entropic attraction of large particles to surfaces. Experiments [11] show not only that large particles segregate at surfaces but that they do so at sufficient density to produce a crystalline phase. In the jargon of modern statistical physics, entropic forces cause a crystalline large-particle phase to wet a fixed surface.

The above discussion, based on a pair-wise attractive interaction between large spheres would lead one to expect that large and small particles would phase separate with increasing volume fraction. The experimental situation is more complicated. Under appropriate conditions, equilibrium crystalline alloys [12,13] of large and small crystals, sometimes with very large unit cells (e.g. AB_{13}), can form. The entropic mechanism for this effect is clear. If the large spheres form a one-component, nearly close-packed lattice, all of the volume between large spheres is denied to the large spheres. A slight expansion of the large-sphere lattice to allow entry of small spheres into its open spaces can enhance the small-sphere entropy.

In the nematic liquid-crystalline phase [14], the long axes of bar-like molecules (Fig. 2a) called *nematogens* align on average along a common direction specified by a unit vector \mathbf{n} called the director. Their centers of mass are, however, randomly distributed as in an isotropic fluid. As first pointed out by Onsager [15], the existence and stability of this phase is due in large part to entropy. A hard rod has both translational and rotational entropy. Motion of randomly positioned and oriented match sticks in a box of fixed volume is strongly inhibited even at a relatively small volume fraction. The same is true for molecules. At high volume fractions, far more translational motion is possible if all of the molecules align along a common direction. The formation of the aligned nematic phase results from an increase in translational entropy that exceeds the reduction of rotational entropy produced by molecular alignment. Using a variational approach, Onsager calculated that isotropic and nematic phases of solutions of spherocylinders of length L and diameter D coexist at respective volume fractions $\phi_i = 3.3D/L$ and $\phi_n = 4.2D/L$.

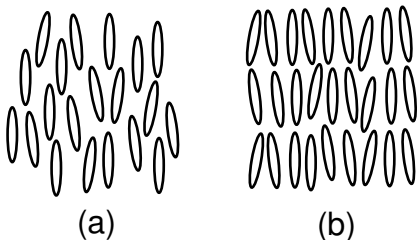


FIG. 2. Schematic representation of (a) the nematic liquid crystalline phase in which rod-like molecules (nematogens) align along a common direction while their centers of mass diffuse freely as in a fluid and (b) the smectic-A phase in which molecular centers of mass segregate into a one-dimensional stack of two-dimensional fluid layers with molecular axes aligned on average along the layer normals.

Our experience with matches (or perhaps the childhood game “pick-up-sticks”) makes the Onsager explanation for the existence of the nematic phase extremely plausible. What is more surprising is that hard-rod entropy also leads to the smectic phase (Fig. 2b) in which the molecular centers of mass segregate into a one-dimensional stack of two-dimensional fluid layers. This result, predicted by computer simulations [16], has been verified by experiments [17] on solutions of tobacco mosaic viruses, which are almost ideal rigid rods. Small spherical particles added to a solution of hard rods induce an attractive depletion force between the rods. However, as in the case of mixtures of two different size spheres, mixtures of rods and spheres can lead to periodic structures with complex multi-particle unit cells [18].

A. Nematic Liquid Crystals: A Tutorial Example

Nematogens can be viewed as long rods. At high temperature or low density, these molecules rotate freely about all axes and form a homogeneous, isotropic fluid. In the nematic phase, the molecules align along a uniform director, which can point in an arbitrary direction. The isotropic phase is invariant under arbitrary translations and rotations, i.e., under all of the operations of the Euclidean group. The nematic phase picks out a particular direction for molecular alignment. It is still invariant under arbitrary translations, but it is invariant only under rotations about the axis parallel to \mathbf{n} . The nematic phase has lower symmetry than the isotropic phase: it is a *broken-symmetry* phase.

This reduction in symmetry can be quantified by an *order parameter* that is nonzero in the nematic phase and zero in the isotropic phase. A convenient order parameter, Q_{ij} , for the nematic phase can be defined as follows. Let ν_i be the unit vector specifying the direction of the long axes of the nematogens. Then $Q_{ij} = \langle \nu_i \nu_j - \frac{1}{3} \delta_{ij} \rangle = S(n_i n_j - \frac{1}{3} \delta_{ij})$ where $\langle \rangle$ denotes an equilibrium ensemble average and $S = \frac{1}{2}(3(\nu \cdot \mathbf{n})^2 - 1)$. This order parameter reflects a broken rotational symmetry, yet like the nematic phase, it is invariant under the inversion operation, $\mathbf{n} \rightarrow -\mathbf{n}$. Different directions of \mathbf{n} define different ordered equilibrium states. Transformations between these states are produced by rotations (through some angle θ), which are symmetry operations of the isotropic phase. The order parameter Q_{ij} transforms under the $l = 2$ irreducible representation of the rotation group.

Since there is no energetically favored direction for \mathbf{n} , uniform rotations of a nematic will not change its free energy F . Spatially nonuniform distortions will, however, increase F . Since the energy of these distortions must go to zero with wavenumber \mathbf{q} , F can be expanded in a power series in gradients of \mathbf{n} . The result is the Frank free energy

$$\begin{aligned}
 F_n &= \frac{1}{2} \int d^3x \{ K_1 (\nabla \cdot \mathbf{n})^2 + K_2 [\mathbf{n} \cdot (\nabla \times \mathbf{n})]^2 \\
 &\quad + K_3 [\mathbf{n} \times (\nabla \times \mathbf{n})]^2 \} \\
 &\approx \frac{1}{2} K \sum_{\mathbf{q}} q^2 |\delta \mathbf{n}(\mathbf{q})|^2,
 \end{aligned} \tag{1}$$

where K_1 , K_2 , and K_3 are rigidity moduli or elastic constants associated, respectively, with splay, twist, and bend distortions of the nematic. The elastic constants have units of force and have a typical magnitude of order 5×10^{-7} dynes. The second form of F is the harmonic limit with $\mathbf{n} \approx (\delta n_x, \delta n_y, 1)$ and equal elastic constants ($K_1 = K_2 = K_3 = K$). This free energy implies a number of important properties of the nematic

state. First, there are low-energy distortions of the nematic phase with energies $\epsilon_q = Kq^2$. The dependence of this energy on q^2 is a direct consequence of the fact that the nematic phase breaks a continuous (rotational) symmetry. Second, the equipartition theorem states that fluctuations in \mathbf{n} satisfy $\langle |\delta\mathbf{n}(\mathbf{q})|^2 \rangle = k_B T / Kq^2$. These fluctuations reduce order and tend to restore rotational isotropy. If K were zero, fluctuations in \mathbf{n} would diverge and destroy nematic order. Thus, the existence of the broken-symmetry nematic state requires the existence of a nonzero rigidity K . Finally, the nematic phase can transmit torques $\tau_i = \delta F / \delta n_i = -K \nabla^2 \delta n_i$ even though it cannot support shear stresses as a solid can.

The broken continuous symmetry leads to the existence of new low-frequency dynamical modes [19,20] in addition to low-energy static excitations. This is the Goldstone theorem [21]. An isotropic fluid has five hydrodynamic modes (positive and negative frequency longitudinal sound, two velocity diffusion, and one energy diffusion mode) associated with the five conservation laws for mass, energy, and momentum. A nematic has two additional director modes (which mix with velocity diffusion modes) associated with the two independent directions that a nematic can be rotated. There is a frictional resistance, characterized by a friction coefficient $\gamma \approx 0.1$ poise with units of viscosity, to the rotation of the director. The simplified hydrodynamic equation for the director is $\partial n_i / \partial t = (K/\gamma) \nabla^2 n_i$ yields a characteristic frequency $\omega \sim Kq^2/\gamma$. The diffusion constant $D_n = K/\gamma$ for this modes is of order $5 \times 10^{-6} \text{cm}^2/\text{s}$ and is much less than the diffusion constant for transverse velocity $D_v = \eta/\rho \approx 10^{-1} \text{cm}^2/\text{sec}$, where $\eta \approx 0.1$ poise is the shear viscosity and $\rho \approx 1 \text{gm}/\text{cm}^3$ is the mass density.

B. General Properties

The nematic example just discussed exhibits properties common to all broken-symmetry phases. Low-symmetry phases typically evolve from higher-symmetry phases from which they can be distinguished by an order parameter, which transforms under some irreducible representation of the symmetry group \mathcal{G} of the higher-symmetry phase. If the low-symmetry phase breaks a continuous symmetry, there are a continuum of states all with the same free energy. These states can be transformed into each other under operations in \mathcal{G} . They can be distinguished from each other by some continuous (possible multi-dimensional) parameter u (such as a rotation angle θ .) Spatially uniform increments in u cost no energy. Spatially nonuniform distortions of u lead to an energy cost $F \sim K \int d^d x (\nabla u)^2$, characterized by a rigidity modulus K and implying an excitation energy $\epsilon_q = Kq^2$. Thermal fluctuations $\langle |u(\mathbf{q})|^2 \rangle = k_B T / Kq^2$ tend to destroy order. Associated with each independent parameter u , there is an additional low-frequency hydrodynamic mode. We will now consider two other examples

of broken-symmetry systems.

C. Smectic Liquid Crystals

The smectic- A phase can be viewed as a one-dimensional periodic stack of fluid layers of aligned nematogens. The ideal smectic phase is distinguished from the nematic phase by a periodic modulation of the mass density parallel to the director \mathbf{n} . Thus, an order parameter for the smectic phase with layers perpendicular to the z -axis can be defined via the Fourier transformation of the density:

$$\rho(\mathbf{x}) = \rho_0 [1 + \psi e^{iq_0[z - u(\mathbf{x})]} + \text{c.c.} + \dots], \quad (2)$$

where $q_0 = 2\pi/d$ and d is the layer spacing. The order parameter $\psi = |\psi| e^{-iq_0 u}$ is the lowest-order complex mass-density-wave amplitude. In general, higher-order Fourier components ψ_n are needed to describe completely a periodic mass density. However, the first component is sufficient for most smectics. The phase variable u distinguishes different equivalent energy states: it translates the origin of periodic modulations.

The smectic free energy depends on gradients of u , and one might expect it to be proportional to $(\nabla u)^2$. This guess is, however, too naive. The smectic free energy must be invariant not only with respect to spatially uniform translations but also with respect to uniform simultaneous rotations of the nematic director \mathbf{n} and the smectic layers. This requirement leads to the free energy

$$F = \frac{1}{2} \int d^3 x [B(\nabla_{\parallel} u)^2 + D(\nabla_{\perp} u + \delta\mathbf{n})^2] + F_n, \quad (3)$$

where \parallel and \perp refer, respectively, to directions parallel and perpendicular to the z axis and F_n is the Frank free energy of Eq. (1). The combination $(\nabla_{\perp} u + \delta\mathbf{n})^2$ is invariant under simultaneous rotations of layers and the director, whereas $(\nabla_{\perp} u)^2$ alone is not. The smectic- A phase breaks both rotational and translational symmetry. One might, therefore, expect three low-energy broken-symmetry modes associated with u , δn_x and δn_y . This is, however, not the case. The presence of periodic order makes it energetically costly to rotate the director relative to the layer normal: there is a finite energy cost $\approx (D + Kq^2) |\delta\mathbf{n}|^2$ as $q \rightarrow 0$ associated with director distortions at $\nabla u = 0$. Layers expel director bend and twist. This phenomenon is identical to the Higgs mechanism [22] for generating a massive Higgs particle in quantum field theory. It is also identical to the expulsion of magnetic flux in a superconductor.

If there are spatial modulations of u , the lowest energy configuration for $\delta\mathbf{n}$ is $\delta\mathbf{n} \approx -\nabla_{\perp} u$. Relaxing $\delta\mathbf{n}$ to this value yields the Landau-Peierls free energy for a one-dimensional solid,

$$F = \frac{1}{2} \int d^3 x [B(\nabla_{\parallel} u)^2 + K_1 (\nabla_{\perp} u)^2], \quad (4)$$

leading to fluctuations, $\langle |u(\mathbf{q})|^2 \rangle = k_B T / (Bq_{\parallel}^2 + K_1 q_{\perp}^4)$. These fluctuations are so strong that the local value of $\langle u^2(\mathbf{x}) \rangle = \int (d^3q / (2\pi)^3) \langle |u(\mathbf{q})|^2 \rangle$ diverges logarithmically with sample size. Thus fluctuations destroy the ideal long-range order of the smectic-*A* phase: $\langle \psi \rangle = |\psi| \langle e^{-iq_0 u} \rangle = |\psi| \exp[-q_0^2 \langle u^2 \rangle / 2] = 0$. Even though ψ is zero at any finite temperature, the smectic phase is distinct from the nematic phase. The rigidity B is nonzero in the smectic phase and zero in the nematic phase. In the nematic phase, correlations in $\psi(\mathbf{x})$ die off exponentially with distance. In the smectic phase, they die off algebraically [23]:

$$\langle \psi(\mathbf{x}) \psi^*(0) \rangle \sim \begin{cases} x_{\parallel}^{-n^2 \eta_c}, & \text{if } \mathbf{x}_{\perp} = 0; \\ |x_{\perp}|^{-2n^2 \eta_c}, & \text{if } x_{\parallel} = 0, \end{cases} \quad (5)$$

where

$$\eta_c = \frac{q_0^2 k_B T}{8\pi (K_1 B)^{1/2}}. \quad (6)$$

The power-law form of spatial correlations implies that the X-ray structure factor will have a power-law rather than a delta function singularity at $\mathbf{q} = n\mathbf{q}_0$:

$$I(\mathbf{q}) \begin{cases} (q_{\parallel} - nq_0)^{-2+n^2 \eta_c}, & \text{if } \mathbf{q}_{\perp} = 0; \\ q_{\perp}^{-4+2n^2 \eta_c}, & \text{if } q_{\parallel} = 0. \end{cases} \quad (7)$$

This behavior has been observed both in single-component smectics [24] and in smectic phases in water-surfactant mixtures [25].

The existence of a single elastic variable u implies the existence of a single additional hydrodynamic mode in a smectic compared to an isotropic fluid. The nature of this mode is quite interesting and contrary to intuition based on harmonic solids. If a smectic is translated with uniform velocity along the z axis, then the time rate of change of the phase variable u will be identical to v_z . In non-equilibrium situations $\partial u / \partial t$ can differ from v_z . In other words, it is possible for molecules to flow relative to a fixed smectic lattice. This is the phenomenon of permeation [26]. There is a dissipative force opposing permeation:

$$\frac{\partial u}{\partial t} - v_z = -\zeta \frac{\delta F}{\delta u} = \zeta (B \nabla_{\parallel}^2 - \nabla_{\perp}^4) u, \quad (8)$$

where ζ is the permeation dissipative coefficient. The equation for the velocity \mathbf{v} couples to u :

$$\rho \frac{\partial v_i}{\partial t} = -\nabla_i p - \delta_{iz} \frac{\delta F}{\delta u} - \eta \nabla^2 v_i. \quad (9)$$

These equations imply the existence of propagating shear modes with frequencies $\omega = \pm \sqrt{B/\rho} (q_x^2 q_z^2 / q^2)$ if q_x and q_z are both nonzero. At $q_x = 0$, there is a pure permeation mode with $\omega = -i\zeta B q_z^2$ in addition to two transverse shear modes.

D. Blue Phases

Liquid crystalline blue phases [27] are remarkable. They are periodic crystalline phases that Bragg scatter in the visible implying unit cell dimensions of order the wavelength of light and, therefore, an enormous number of molecules per unit cell. Even more surprising is that there is no discernible modulation in their mass density. Rather there is a periodic modulation in the nematic order parameter Q_{ij} specifying the magnitude and direction of orientational order. Blue phases are, nonetheless, true periodic crystals that support shear [28] and form faceted surfaces [29] when they coexist with the isotropic phase. Order parameters for the Blue phases can be obtained from the Fourier expansion of Q_{ij} :

$$Q_{ij}(\mathbf{x}) = \sum_{\mathbf{G}} Q_{ij}^{\mathbf{G}} e^{i\mathbf{G} \cdot (\mathbf{x} - \mathbf{u})}, \quad (10)$$

where \mathbf{G} is a reciprocal lattice vector of the cubic lattice. The complex tensor amplitude $Q_{ij}^{\mathbf{G}} e^{-i\mathbf{G} \cdot \mathbf{u}}$ are the blue-phase order parameters.

The energy of a blue phase is invariant with respect to uniform translations of \mathbf{u} and with respect to simultaneous rigid rotations of the lattice and the anisotropic molecules. As in a smectic, the latter invariance introduces couplings between molecular rotation through angles Ω_i and lattice rotations through angles $\omega_i = \epsilon_{ijk} \partial_j u_k / 2$ of the form $(\omega_i - \Omega_i)^2$ and causes molecular rotation relative to a fixed lattice to be energetically costly. This is the Higgs mechanism again. As a result, ω_i locks to Ω_i at long wavelengths, and the long wavelength elastic energy depends only on the symmetrized strain tensor $u_{ij} = (\partial_i u_j + \partial_j u_i) / 2$ and has a form [30] identical to that of any cubic crystal:

$$F_{\text{el}} = \frac{1}{2} \int d^3x K_{ijkl} u_{ij} u_{kl}, \quad (11)$$

where K_{ijkl} is the elastic constant tensor with 3 independent components in a cubic crystal. The cubic anisotropy of the blue phases is small, and F_{el} can be approximated by the elastic energy of an isotropic solid with Lamé coefficients λ and μ . The shear modulus μ is of order a Frank elastic constant divided by the square of the lattice parameter $d \approx 2000 \text{ \AA}$: $\mu \approx K/d^2 \approx 5 \times 10^{-7} / (2 \times 10^{-5})^2 = 10^3 \text{ dynes/cm}^2$. It is 10^9 times smaller than the shear modulus of a typical hard solid like aluminum.

The equations [30] governing the long wavelength hydrodynamics of a blue phase are identical to those [20] of any cubic crystal, hard or soft. The softness of the blue phases, however, leads to a mode structure not found in hard systems. There are three hydrodynamic variables u_x , u_y , and u_z , not present in an isotropic fluid. There are, therefore, a total of 8 hydrodynamical modes: two longitudinal sound modes, four transverse sound, one heat diffusion, and one vacancy diffusion mode. Vacancy diffusion is really mass motion relative to a fixed periodic lattice: it is the same thing as permeation. In hard

crystals, vacancy diffusion is a very slow activated process and can often be ignored. In soft crystals, especially in large unit cell structures, it cannot be. In addition propagating shear modes can become overdamped permeation-velocity modes above a critical wavenumber. The displacement \mathbf{u} and the velocity \mathbf{v} obey vector versions of the permeation and force equations, Eqs. (8) and (9). The magnitude [26,30] of the dissipative coefficient ζ is of order $d^2/[(2\pi)^2\gamma]$, where γ is the friction coefficient of a nematic liquid crystal. These equations predict a diffusive longitudinal permeation mode with diffusion coefficient $D_p = \zeta\mu \approx (2\pi)^{-2}K/\gamma \approx 10^{-7}\text{cm}^2/\text{s}$ or about an order of magnitude smaller than the director diffusion coefficient of the nematic and six orders of magnitude smaller than the velocity diffusion coefficient D_v . Since D_p/D_v is so small, it can be ignored in the equation for shear displacements, which then obeys the standard damped shear-wave equations: $\rho\partial_t^2\mathbf{u} = -\nabla^2(\mu + \eta\partial_t)\mathbf{u}$. At the longest wavelengths, there is a propagating damped shear mode with velocity $c = \sqrt{\mu/\rho} \approx 30\text{cm}/\text{sec}$. At wavenumbers greater than $q_c = 2c/D_v = 2\sqrt{\mu\rho}/\eta \approx 500\text{cm}^{-1}$ for $\eta \approx 0.1$ poise, dissipation dominates, and the shear wave breaks up into two over-damped and diffusive-like modes. The critical wavenumber q_c is of order 10^{-4} times smaller than the zone edge vector $2\pi/d \approx 3 \times 10^6\text{cm}^{-1}$. Thus, the shear mode is overdamped over most of the Brillouin zone. Similar behavior occurs in colloidal crystals.

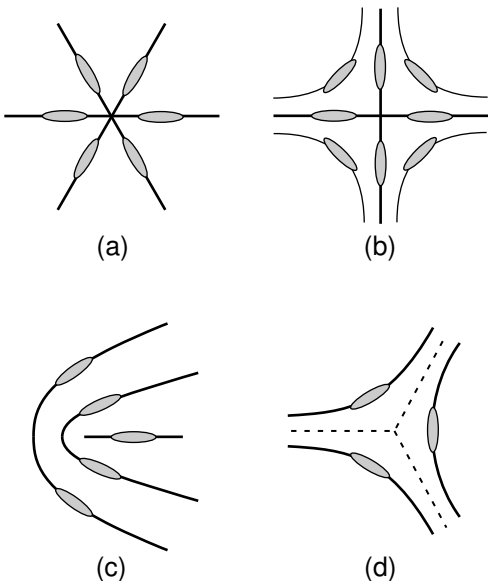


FIG. 3. Director configuration for disclinations in two-dimensions with (a) $k = 1$, (b) $k = -1$, (c) $k = 1/2$, and (d) $k = -1/2$.

IV. TOPOLOGICAL DEFECTS

Consider a two-dimensional nematic for which the director can be written as $\mathbf{n} = (\cos\theta, \sin\theta)$. This system can have a special kind of defect, called a disclination, in

which θ changes by $2k\pi$, where k is a half-integer, in one circuit around a point core as shown in Fig. 3. The order parameter Q_{ij} is continuous and well defined everywhere except at the core, even though θ undergoes a discontinuous change of $-k\pi$ along some line originating at the core. A disclination is one of a class of what are called topological defects [31]. These defects have the property that no continuous distortion can make them disappear (i.e., return the system to its undistorted aligned ground state). Their properties depend on the symmetry of the order parameter and the topological properties of the space in which the transformation variable θ resides (the unit circle with opposite points identified in the case of the two-dimensional nematic). Examples of topological defects include vortices in superfluid helium and in superconductors, dislocations and disclinations in crystals and liquid crystals, and hedgehogs in magnets and nematic liquid crystals.

Topological defects play a determining role in a number of physically important phenomena. The proliferation of vortices is responsible for the transition from the superfluid to the normal state in helium films. Dislocations determine the strength of crystals. The Abrikosov phase in superconductors is a lattice of vortices.

Soft condensed matter systems are ideal for the study of topological defects. As discussed in the preceding section, soft systems are characterized by easy response to external forces and by characteristic lengths much larger than a molecular scale. This makes it possible not only to produce defects in a controlled way via boundary conditions and external fields but also to produce defects with length scales that can be imaged simply with optical techniques. In the next two subsections, we will give some examples of topological defects in soft systems.

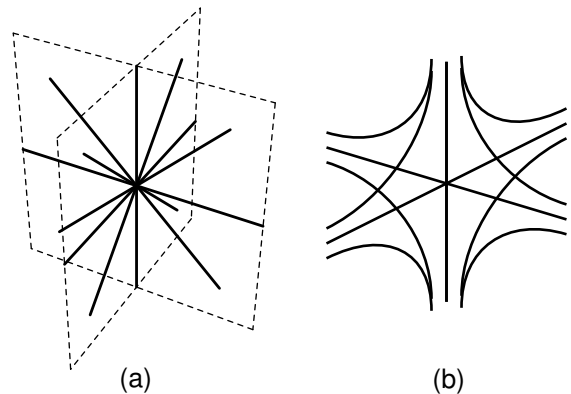


FIG. 4. Director configurations for (a) a radial hedgehog with $Q = \pm 1$ and (b) a hyperbolic hedgehog with $Q = \pm 1$. The sign of the hedgehog in a nematic is ambiguous because of the $\mathbf{n} \rightarrow -\mathbf{n}$ symmetry

A. nematic liquid crystals

As we just saw, a two-dimensional nematic can have point topological defects called disclinations. In three-

dimensional nematics, there are strength $1/2$ disclination line defects around which the director rotates by $(2\pi)/2$. In addition, there are point defects called hedgehogs (Fig. 4) characterized by a topological charge Q . In the simplest $Q = 1$ hedgehog, the director points radially outward like the electric field around a point charge. A $Q = 1$ hyperbolic hedgehog is obtained from the radial hedgehog by rotating all vectors through π about the z axis. At low temperature, there will be a small number of thermally activated disclination loops and hedgehogs. As temperature increases, the number and size of these defects will increase. At sufficient density, they will destroy the order of the nematic phase. The isotropic phase can thus be modeled as a nematic phase riddled with disclinations and hedgehogs. Experimental verification [32] of this picture can be obtained by suddenly quenching an isotropic phase to a temperature at which the nematic phase is stable. A spaghetti of disclination lines is visible shortly after the quench. As time goes on, the disclination density decreases via annihilation processes. Interestingly, the characteristic distance between disclinations increase as a power law in time at long times. This quenching into the nematic phase provides a useful model for the formation of cosmic strings [32].

Another interesting example of topological defects in nematics is provided by nematic emulsions. If nematogens are mixed in water with a surfactant, they will form essentially spherical emulsion droplets [33] with diameters ranging from $0.5\mu\text{m}$ to $50\mu\text{m}$ and more. Boundary conditions at the surface of the droplet depend on the surfactant, and both normal and tangential boundary conditions can be produced. Normal boundary conditions [31] force the creation of a $+1$ hedgehog at the center of the droplet. Tangential boundary conditions lead to surface defects called boojums [34]. The defect state can be modified by external electric or magnetic fields. Since the way a droplet scatters light depends on its director configuration, different topological states will scatter light differently. It is thus possible to control the amount of light scattering from an array of droplets with modest electric fields. This is the basis for a display technology [33].

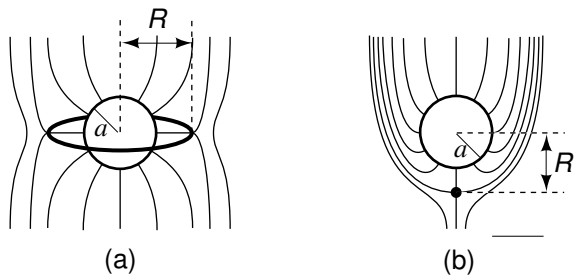


FIG. 5. (a) “Saturn Ring” configuration of a spherical particle with normal boundary conditions in a nematic. A disclination ring screens the radial hedgehog created by the particle producing parallel alignment at long distances. (b) Dipole configuration in which the additional particle creates a hyperbolic hedgehog.

If small water droplets favoring director alignment normal to their surfaces are dispersed in a nematic, they will nucleate a hedgehog [35]. If fields or boundary conditions force average alignment of the nematic along some direction, the total hedgehog number must be zero. Thus, each water droplet must create a compensating companion defect such as depicted in Fig. 5. If the diameter of the water droplet is of order a micron or larger, the compensating defect is a hyperbolic hedgehog as shown in Fig. 5b. This defect leads to a short-range repulsion between droplets that prevents coalescence. The droplet-defect pair form a dipole configuration that disrupts the far-field director and leads to an attractive interaction between aligned dipoles. The result is that water droplets in a nematic form chains just like magnetic dipoles with short-range repulsion. Smaller droplets may nucleate a disclination ring about their equator [36] in the “Saturn ring” configuration shown in Fig. 5a.

B. Smectic Liquid Crystals

Dislocations in smectics are topological defects in which u undergoes a change of kd , where k is an integer and d is the smectic layer spacing, in one circuit around a linear core. Dislocations form when a smectic is forced into geometric environments that are incompatible with its layered structure. For example there must be dislocations in a smectic wedged between two nonparallel surfaces if boundary conditions force the director to be normal to those surfaces.

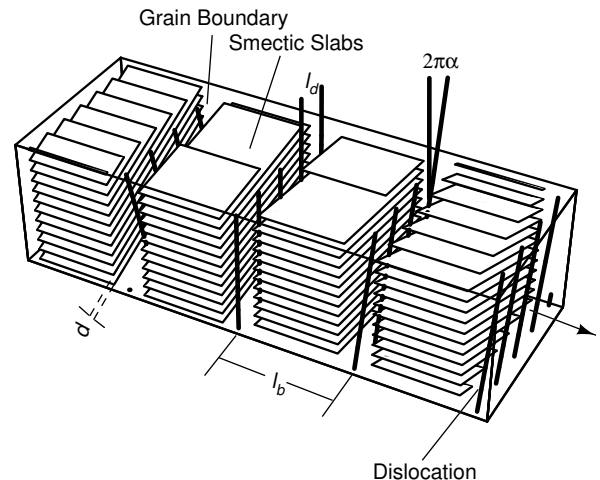


FIG. 6. Schematic representation of the TGB phase showing smectic slabs separated by grain boundaries composed of periodically spaced screw dislocations. The change in angle of the smectic layer normal across a grain boundary is $2\pi\alpha = 2 \sin^{-1} d/2l_d$ where d is the layer spacing and l_d is the separation between dislocations. If α is a rational number P/Q for relatively prime integers P and Q , the structure has a Q -fold screw axis and quasicrystalline symmetry if $Q = 5$ or $Q > 6$. If α is irrational, the structure is rotationally incommensurate.

A particularly beautiful example of topological defects in smectic liquid crystals is the twist-grain-boundary or TGB phase [37] shown in Fig. 6. Chiral molecules prefer twisted to parallel structures. If chirality is added to a nematic liquid crystal, a twisted nematic or cholesteric phase results in which $\mathbf{n} = (\cos k_0 z, \sin k_0 z, 0)$ rotates in a helical fashion about a pitch axis. This twisting structure is incompatible with the periodic layering of the smectic phase. Thus the smectic either expels twist altogether, or it permits twist via the formation of a regular lattice of grain boundaries, each composed of a periodic array of screw dislocations, across which the smectic layers undergo a discrete rotations. The smectic phase is analogous the superconducting phase, and the nematic-to-smectic-*A* transition is analogous to the the normal-to-superconduction transition [38]. Twist is the analog of the *B* field in a superconductor. The TGB phase is the analog of the Abrikosov vortex lattice phase and the smectic phase with expelled twist is the analog of the Meissner phase in superconductors. TGB phase have been found in a large number of compounds [39]. There are even quasicrystalline [40] TGB phases with 16- to 20-fold screw axes.

V. MEMBRANES

Membranes [41] are two-dimensional flexible surfaces. Aliphatic molecules, such as detergents and biologically important phospholipids, are molecules with a polar hydrophilic (water-loving) head and a hydrocarbon hydrophobic (water-fearing) flexible tail. When these molecules are dissolved in water, they spontaneously form structures that protect the hydrocarbon tail from contact with water. At sufficient concentration, they form large, bilayer membranes that can assume a variety of shapes including nearly flat surfaces, closed vesicles with the topology of a sphere, and more complex multi-connected surfaces similar to the Fermi surface of copper. These membranes are both flexible and fluid: their shape changes easily, and their constituent molecules diffuse freely within the confines of the surfaces they define. They are perfect examples of soft materials.

In its lowest energy state, the membrane defines a flat surface that breaks the translational and rotational symmetry of space. If the fluid membrane is free and not under tension, the energy of deformed states is determined by the Helfrich-Canham [42] free energy:

$$F_{\text{mem}} = \frac{1}{2}\kappa \int dS \left(\frac{1}{R_1} + \frac{1}{R_2} \right)^2 \approx \frac{1}{2}\kappa \int dS (\nabla^2 h)^2, \quad (12)$$

where R_1 and R_2 are the local radii of curvature, $R_1^{-1} + R_2^{-1}$ is the local mean curvature, and κ is a bending rigidity with units of energy. The second form of this energy is the harmonic expansion about the flat surface with

points on the membrane parametrized by their height $h(x, y)$ above the xy plane. The rigidity κ has values that range from one to several tens of $k_B T$. F_{mem} is invariant with respect to both uniform translations and rotations. The layer normal is $\mathbf{N} \approx (-\partial_x h, -\partial_y h, 1)$ for small ∇h . Thus ∇h describes a rotation of \mathbf{N} , which cannot change the membrane energy. There can be no $(\nabla h)^2$ contribution of F_{mem} , and the leading contribution is $(\nabla^2 h)^2$. A membrane has all of the modes of a two-dimensional fluid (two-dimensional sound and heat and momentum diffusion) plus a height mode with a long-wavelength energy $\epsilon_q = \kappa q^4$ proportional to q^4 (rather than $\sim q^2$) because both translational and rotational symmetry are broken. The latter mode dissipates energy into the shear modes of the surrounding fluid. It is overdamped with a frequency ω_q that must decrease with increasing fluid viscosity η . Dimensional analysis then implies that $\omega_q \sim (\kappa/\eta)q^3 \approx 10^4 \text{Hz}$ at $\lambda = 2\pi/q \approx 2000 \text{\AA}$. Thermal height fluctuations $\langle |\delta h(\mathbf{q})|^2 \rangle = k_B T / \kappa q^4$ diverge strongly at small q and lead to a decorrelation of layer normals. A persistence length L_p beyond which orientational memory is lost can be defined as the length at which the layer-normal correlation function,

$$\begin{aligned} \langle [\mathbf{N}(\mathbf{x}) - \mathbf{N}(0)] \rangle &= \frac{k_b T}{\kappa} \int \frac{d^2 q}{(2\pi)^2} \frac{1 - e^{i\mathbf{q}\cdot\mathbf{x}}}{q^4} \\ &= \frac{k_B T}{2\pi\kappa} \ln |\mathbf{x}|/\xi, \end{aligned} \quad (13)$$

becomes of order unity [43]. This yields $L_p = \xi e^{2\pi\kappa/k_B T}$. At length scales beyond L_p a free membrane will no longer be flat; it will assume complicated crumpled configurations.

Fluid membranes are the basic constituents of a number of thermodynamically stable phases of which the simplest is the lyotropic lamellar phase formed by a periodic stack of membranes separated by water. This phase is a smectic liquid crystalline phase with a layer spacing d that can be varied from 50\AA to several microns. There is a negative interfacial energy per unit area σ that favors large membrane area. This is opposed by interactions between membranes. When charges are fully screened, membranes interact only when they are in close contact. Height fluctuations of a membrane confined between two others will be smaller than those of a free membrane. The confined membrane has a lower entropy than a free membrane. As a result, there will be an entropic repulsion between membranes. The balance between the attractive interfacial force and the entropic repulsive entropic force determines the equilibrium layer spacing and the elastic compression modulus B . Helfrich [44] provided an estimate of the entropy reduction as follows. A fluctuating membrane will collide with its neighbors as depicted in Fig. 7. The mean-square height fluctuation will be of order d^2 at a length scale of order L_B , the mean distance between collisions in the xy plane:

$$d^2 = \langle h^2(\mathbf{x}) \rangle \approx \frac{k_B T}{\kappa} L_B^2. \quad (14)$$

Each collision leads to an entropy reduction of order k_B . There are $N = V/(L_B^2 d)$ collisions in a volume d . Thus the entropy reduction per unit volume is $\Delta s = -k_B/L_B^2 d$. The gain in free energy per unit volume arising from increased surface area is $-\sigma/d$. Thus the free energy density of a stack of membranes is

$$f = \frac{(k_B T)^2}{\kappa d^3} - \frac{\sigma}{d}. \quad (15)$$

Minimization with respect to d yields $d = (\sigma \kappa / 3 k_B^2 T^2)^{1/3}$ and a compression modulus $B = d^2 \partial^2 f / \partial d^2 = 6 k_B^2 T^2 / \kappa d^3$. X-ray experiments have verified this relation [25]. An almost identical entropic analysis applies to the striped phase of atoms adsorbed onto a graphite substrate [45].

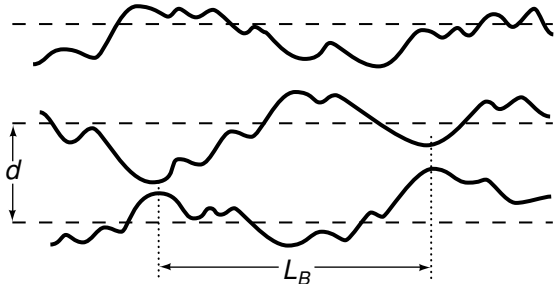


FIG. 7. Representation of a lattice of fluctuating membranes. The average separation between membranes is d . The average distance in the xy plane between collisions is L_B . Between collisions, each membrane is free. The distance d and L_B are related via $d^2 = (k_B T / \kappa) L_B^2$.

Membranes can develop varying degrees of internal order that modify their properties [41]. For example, their constituent molecules can tilt relative to their normals. This breaks rotational symmetry in the plane of the membrane and leads to a vector in-plane orientational order parameter. Or, polymerization can produce a two-dimensional solid with a harmonic shear and bulk modulus but with height fluctuations out of the plane of the membrane. As in a fluid, the latter fluctuations are very soft with energy $\epsilon_q = \kappa q^4$. Coupling between the soft height mode and in-plane shear leads to a remarkable renormalization [46] of the elastic so that the renormalized long-wave-length bending modulus diverges as $q^{-\eta_h}$ and the shear and bulk moduli vanish as q^{η_u} with $\eta_u = 2(1 - \eta_h)$. Non-linearities actually destroy harmonic elasticity!

VI. PROSPECTS FOR THE FUTURE

Soft condensed matter physics is a vast and vibrant field. It will continue to be a growth area for the foreseeable future enriching both physics and the many sciences such as chemistry, chemical engineering, materials science, and biology that it overlaps. Listed below are some

(but certainly not all) areas where one can expect to see exciting progress in the next few years.

A. New Structures

The ease with which soft condensed matter can deform is responsible for such remarkable phases as the TGB phase. There are surely others to be discovered. For example, disc-like (rather than rod-like) molecules or semiflexible polymers tend to form columnar structures in which there is hexagonal crystalline order in two dimensions and fluid-like structure in the third. Chirality in these systems should produce a variety of “braided” and TGB-like structures [47]. A good candidates system to see these phase is aligned DNA. Another structure that may exist is a TGB-blue phase in which smectic layering coexists with a three-dimensional twist structure. The ability of synthetic chemists to engineer molecules with exotic shapes plays an important role in this arena.

B. Measurement and Control at the Micron Scale and Lower

A variety of new or improved experimental techniques, including laser and magnetic tweezers and fluorescence and near-field microscopy make it possible both to visualize and to control processes at the micron scale and lower. For example, laser tweezers can be used to confine colloidal particles to specified regions, to move them about, and to measure piconewton forces. One can expect to see an explosion of new experimental data on a variety of systems. Examples of experiments that have already been done include the measurement of extension versus force on DNA [48], the effect of depletion forces on diffusion in controlled geometries [49], and the laser induction of pearling instabilities in bilayer cylindrical vesicles [50]. More will follow.

This new control will also lead to new materials. In the near future, we should see designer two- and three-dimensional colloids engineered through clever use of surface templates, depletion forces, laser tweezers, and related techniques. Interesting new materials would be optical band gap materials in the form of a regular 3D lattice of low and high dielectric constant spheres or a 3D crystal of two different size nematic emulsion droplets.

Nanoscale phenomena is a hot subject in hard (electronic) as well as soft condensed matter physics. Soft condensed matter will be used to create templates for the creation of metallic nanostructures.

C. Biology

One of the most exciting areas of soft condensed matter physics is its interface biology. The fundamental build-

ing blocks, the plasma membrane, the cytoskeleton, microtubules, DNA and actin molecules, etc., are soft materials. They have mechanical properties that are well described by the language presented in this article: They are polymers or surfaces with differing rigidities; they are subject to depletion forces and viscous forces when they move, etc. Soft condensed matter physics will have an increasing impact on biology and conversely biology, by providing examples of how nature creates and uses structures, will provide paradigms for new soft materials.

I am pleased to dedicate this article to Eli Burstein on the occasion of his 80th birthday. His love of and commitment to all physics, and condensed matter physics in particular, has been an inspiration to us all.

The author is grateful to Arjun Yodh and David Weitz for useful conversations. This work was supported in part by grants from NSF under grant No. DRM94-23114 and DMR91-22645.

-
- [1] For a more detailed and pedagogical account of many of the items presented here, see P.M. Chaikin and T.C. Lubensky, *Principles of Condensed Matter Physics* (Cambridge University Press, Cambridge, 1995).
- [2] Pierre-Gilles de Gennes, *Scaling Concepts in Polymer Physics* (Cornell University Press, Ithaca, 1979).
- [3] See for example W.B. Russel, D.A. Saville, and W.R. Schowalter, *Colloidal Dispersions* (Cambridge University Press, Cambridge, 1989).
- [4] There are of course many random-close-packed configurations that are ultimately responsible for the “ground state entropy” of a glass. Different configurations are, however, inaccessible to hard spheres at true close packing, and we may take the entropy of a single configuration to be zero.
- [5] W.G. Hoover and F.H. Ree, *J. Chem. Phys.* **49**, 3609 (1968); B. J. Alder, W.G. Hoover, and D.A. Young, *ibid.* **49**, 3688 (1968).
- [6] See for example, P.N. Pusey and W. van Meegen, *Nature (London)* **320**, 340 (1986); S.E. Paulin and B.J. Ackerson, *Phys. Rev. Lett.* **64**, 2663 (1990).
- [7] B.J. Ackerson and N.A. Clark, *Phys. Rev. Lett.* **46**, 123 (1981); *Phys. Rev. A* **30**, 906 (1981).
- [8] S. Asakura and F. Oosawa, *J. Chem. Phys.* **22**, 1255 (1954).
- [9] See for example Steven B. Zimmerman and Allen P. Minton, *Annu. Rev. Biomol. Struct.* **22**, 27 (1993); Judith Herzfeld, *Acc. Chem. Res.* **29**, 31 (1996).
- [10] H. De Hek and A. Vrij, *J. Colloid Interface Sc.* **84**, 409 (1981); F.L. Calderon, J. Bibette, and J. Biais, *Europhys. Lett.* **23**, 653 (1993); S.M. Ilett, A. Orrock, W.C.K. Poon, and P.N. Pusey, *Phys. Rev. E* **51**, 1344 (1995).
- [11] P.D. Kaplan, J.L. Rouke, A.G. Yodh, and D.J. Pine, *Phys. Rev. Lett.* **72**, 582 (1994); A.D. Dinsmore, A.G. Yodh, and D.J. Pine, *Phys. Rev. E* **52**, 4045 (1995).
- [12] P. Bartlett, R.H. Ottewill, and P.N. Pusey, *Phys. Rev. Lett.* **68**, 3801 (1992); J.V. Sanders, *Philos. Mag. A* **42**, 705 (1980); S. Yoshimura and S. Hachisu, *Prog. Colloid Polym. Sci.* **68**, 59 (1983).
- [13] M.D. Eldridge, P.A. Madden, and D. Frenkel, *Molec. Phys.* **79**, 105 (1993); H. Xu and M. Baus, *J. Phys. Condensed Matter* **4** L663 (1993).
- [14] P.G. de Gennes and J. Prost, *The Physics of Liquid Crystals*, 2nd edn (Clarendon Press, Oxford, 1993); S. Chandrasekhar, *Liquid Crystals* (Cambridge University Press, 1992).
- [15] L. Onsager, *Ann. N.Y. Acad. Sci.* **51**, 627 (1949).
- [16] A. Stroobants, H.N.W. Lekkerkerker, and D. Frenkel, *Phys. Rev. A* **36**, 2929 (1987); D. Frenkel in *Phase Transitions in Liquid Crystals*, edited by S. Martellucci and A.N. Chester (Plenum Press, N.Y., 1992).
- [17] X. Wen, R.B. Meyer, and D.L.D. Caspar, *Phys. Rev. Lett.* **63**, 2760 (1989); Seth Fraden in *Observations, Predictions, and Simulations in Complex Fluids*, M. Baus, L.F. Ryll, and J.D. Ryckaert, eds. (Kluwer Academic Publishers, Dordrecht, 1995).
- [18] Seth Fraden, private communication.
- [19] Dieter Forster, *Hydrodynamics, Broken Symmetry, and Correlations Functions* (Addison Wesley, Reading, Mass., 1983).
- [20] P.C. Martin, O. Parodi, and P.S. Pershan, *Phys. Rev. A* **6**, 2401 (1972).
- [21] J. Goldstone, *Nuovo Cimento* **19**, 155 (1961).
- [22] P.W. Higgs, *Phys. Lett.* **12**, 132 (1964), **13**, 508 (1964).
- [23] A. Caillé, *C.R. Acad. Sci. (Paris)* **274** 891 (1972); T.C. Lubensky, *Phys. Rev. Lett.* **29**, 206 (1972).
- [24] J. Als-Nielsen, J.d. Litster, R.J. Birgeneau, M. Kaplan, C.R. Safinya, A. Lindegaard-Andersen, and S. Mathiesen, *Phys. Rev. B* **22**, 312 (1980).
- [25] C.R. Safinya, D. Roux, G.S. Smith, S.K. Sinha, P. Dimon, N.A. Clark, and A.M. Belloq, *Phys. Rev. Lett.* **57**, 2718 (1986); D. Roux and C.R. Safinya, *J. Phys. (Paris)* **49**, 307 (1988).
- [26] W. Helfrich, *Phys. Rev. Lett.* **23**, 372 (1969);
- [27] See for example H. Stegemeyer, Th. Blümel, K. Hiltrop, H. Onusseit, and F. Porsch, *Liq. Cryst.* **1**, 3 (1986); David C. Wright and N. David Mermin, *Rev. Mod. Phys.* **61**, 385 (1989).
- [28] N.A. Clark, S.T. Vohra, and M.A. Handschy, *Phys. Rev. Lett.* **52**, 57 (1984); P.E. Cladis, P. Pieranski, and M. Joanicot, *Phys. Rev. Lett.* **52**, 542 (1984); R. N. Kleiman, D.J. Bishop, R. Pindak, and P. Taborek, *Phys. Rev. Lett.* **53**, 2137 (1984).
- [29] P. Pieranski, R. Barbet-Massin, and P.E. Cladis, *Phys. Rev. A* **31**, 3912 (1985).
- [30] Holger Stark and Hans-Rainer Trebin, *Phys. Rev. E* **51**, 2316 (1995); **51** 2326 (1995).
- [31] Maurice Kléman, *Points, Lines and Walls: in Liquid Crystals, Magnetic systems, and Various Disordered Media* (J. Wiley, New York, 1983); M.V. Kurik and O.D. Lavrentovich, *Usp. fiz. Nauk*, **154**, 381 (1988) [*Sov. Phys. Usp.* **31**, 196 (1988).]; N.D. Mermin, *Rev. Mod. Phys.* **51**, 591 (1979).
- [32] I. Chuang, B. Yurke, A.N. Pargellis, and N. Turok, *Phys. Ref. E*, **47**, 3343 (1993); A.J. Bray, *Physica A* **194**, 41

- (1993).
- [33] P. Draziac, *Liquid Crystal Dispersions* (World Scientific, Singapore, 1995)
 - [34] G.E. Volovik and O.D. Lavrentovich, *Sov. Phys. JETP* **58**, 1159 (1983).
 - [35] Philippe Poulin, Holger Stark, T.C. Lubensky, and D.A. Weitz, submitted to *Science*
 - [36] E.M. Terentjev, *Phys. Rev. E* **51**, 1330 (1995); O.V. Kksenpk, R.W. Ruhwandl, S.V. Shiyanovskii, and E.M. Terentjev, Cambridge preprint.
 - [37] S.R. Renn and T.C. Lubensky, *Phys. Rev. A* **38**, 2132 (1988); J. Goodby, M.a. Waugh, S.M. Stein, E. Chin, R. Pindak, and J.S. Patel, *Nature (London)* **337**, 449 (1988); *J. Am. chem. soc.* **111**, 8119 (1989).
 - [38] P.G. de Gennes, *Solid State Commun.* **10**, 753 (1972).
 - [39] J. W. Goodby, I. Nishiyama, A.J. Slaney, C.J. Booth, K.J. Toyne, *Liq. Cryst.* **14**, 27 (1993); H.T. Nguyen, A. Bouchta, L. Navailles, P. Barois, N. Isaert, R.J. Tieg, A. Maaroufi, C. Destrade, *J. Phys. II (Paris)* **2**, 1889 (1992).
 - [40] L. Navailles, P. Barois, H. Nguyen, *Phys. Rev. Lett.* **72**, 1300 (1994); L. Navailles, P. Barois, R. Pindak, H.T. Nguyen, *Phys. Rev. Lett.* **74**, 5224 (1995).
 - [41] R. Lipowsky, *Nature* **349**, 475 (1991); D.Nelson and S. Weinberg (eds.), *Statistical Mechanics of Membranes and Surfaces* (World Scientific, Singapore, 1989); Samuel A. Safran, *Statistical Mechanics of Membranes and Interfaces* (Addison Wesley, Reading, Mass. 1994).
 - [42] R. Canham, *J. Theor. Biol.* **26**, 61 (1970); W. Helfrich, *Z. Naturforsch* **28C**, 693 (1973).
 - [43] P.G. de Gennes and C. Taupin, *J. Phys. Chem.* **86**, 2294 (1982)
 - [44] W. Helfrich, *Z. Naturforsch.* **33A**, 205 (1978).
 - [45] V.L. Pokrovsky and A.L. Talapov *Phys. Rev. Lett.* **42**, 66 (1979); S.N. Coppersmith, Daniel S. Fisher, B.I. Halperin, P.A. Lee, and W.F. Brinkman, *Phys. Rev. Lett.* **46**, 549 (1981).
 - [46] D.R. Nelson and L. Peliti, *J. Physique* **48**, 1085 (1987); J.A. Aronovitz and T.C. Lubensky, *Phys. Rev. Lett.* **60**, 2634 (1988).
 - [47] Randall D. Kamien and David R. Nelson, *Phys. Rev. Lett.* **74**, 2499 (1995); *Phys. Rev. E* **53**, 650 (1996).
 - [48] S.B. Smith, L. Finzi, and C. Bustamante, *Science* **258**, 1122 (1992); T.R. Strick, J.-f. Allemand, D. Bensimon, A. Bensimon, and V. Croquette, *Phys. Rev. Lett.* **??**, ??? (1996).
 - [49] David Boas and Arjun Yodh, to be published in *Nature*
 - [50] R. Bar-Ziv, T. Frisch, and E. Moses, *Phys. Rev. Lett.* **75**, 3481 (1995).